Journal of Agricultural Engineering

https://www.agroengineering.org/

Estimating rice yield under different wheat residue coverage levels using multispectral Gaofen satellite data and remote sensing indices

Muhammad Sohail Memon,[1,2,3] Shuren Chen,[1,2] Jun Guo,[4] Babar Iqbal,[5] Zhiqiang Du,[1,2] Mohamed Farag Taha,[2,6] Noreena Memon[3]

[1]Key Laboratory of Modern Agricultural Equipment and Technology of Ministry of Education, Jiangsu University, Zhenjiang, China
[2]School of Agricultural Engineering, Jiangsu University, Zhenjiang, China
[3]Department of Farm Power and Machinery, Faculty of Agricultural Engineering and Technology, Sindh Agriculture University, Tandojam, Pakistan
[4]School of Automotive Engineering, Yancheng Institute of Technology, Yancheng, Jiangsu, China
[5]School of Environment and Safety Engineering, Jiangsu University, Zhenjiang, China
[6]Department of Soil and Water Sciences, Faculty of Environmental Agricultural Sciences, Arish University, North Sinai, Egypt

Corresponding authors:
Chen Shuren, School of Agricultural Engineering, Jiangsu University, Zhenjiang 212013, China. E-mail: srchen@ujs.edu.cn
Muhammad Sohail Memon, School of Agricultural Engineering, Jiangsu University, Zhenjiang 212013, China. E-mail: msohail@ujs.edu.cn

---

Please cite this article as doi: 10.4081/jae.2025.1698

Submitted: 10 February 2025
Accepted: 29 May 2025

Estimating rice yield under different wheat residue coverage levels using multispectral Gaofen satellite data and remote sensing indices

Muhammad Sohail Memon,[1,2,3] Shuren Chen,[1,2] Jun Guo,[4] Babar Iqbal,[5] Zhiqiang Du,[1,2] Mohamed Farag Taha,[2,6] Noreena Memon[3]

[1]Key Laboratory of Modern Agricultural Equipment and Technology of Ministry of Education, Jiangsu University, Zhenjiang, China
[2]School of Agricultural Engineering, Jiangsu University, Zhenjiang, China
[3]Department of Farm Power and Machinery, Faculty of Agricultural Engineering and Technology, Sindh Agriculture University, Tandojam, Pakistan
[4]School of Automotive Engineering, Yancheng Institute of Technology, Yancheng, Jiangsu, China
[5]School of Environment and Safety Engineering, Jiangsu University, Zhenjiang, China
[6]Department of Soil and Water Sciences, Faculty of Environmental Agricultural Sciences, Arish University, North Sinai, Egypt

Corresponding authors:
Chen Shuren, School of Agricultural Engineering, Jiangsu University, Zhenjiang 212013, China. E mail: srchen@ujs.edu.cn
Muhammad Sohail Memon, School of Agricultural Engineering, Jiangsu University, Zhenjiang 212013, China. E- mail: msohail@ujs.edu.cn

Abstract

Satellite remote sensing (RS) offers an efficient, large-scale approach for monitoring crop health, particularly in precise estimation of crop yields. Rice is a staple food for over three billion people worldwide, making it crucial to estimate rice yield promptly to ensure food security and support sustainable agriculture. However, traditional field survey methods for yield assessment, are often labor-intensive, and time-consuming. To address this challenge, we propose a novel approach that integrates Gaofen-1 (GF-1) and Gaofen-6 (GF-6) multispectral data for monitoring and evaluating rice crop yield under different wheat residue cover (WRC) percentages. This method employed three Remote Sensing (RS) based vegetation indices (VIs): i) enhanced vegetation index (EVI), ii) normalized difference vegetation Index (NDVI), and iii) green normalized difference vegetation index (GNDVI), with field data collected from 80 sampling points across paddy fields in the Changshu County, China. The results demonstrated that land use and land cover (LULC) mapping effectively classified paddy fields, covering 66% of the study area, with a classification

accuracy of 88% (κ = 0.84). Among the relationships tested between VIs and WRC, NDVI showed the highest correlation (R^2 = 0.66), followed by EVI (R^2 = 0.60) and GNDVI (R^2 = 0.51), confirming NDVI as the most effective index for yield modeling. The yield estimation model, based on peak NDVI values correlated with measured rice yield from the calibration dataset (n=52), achieved R^2 = 0.83, and validation with test data (n=28) showed high accuracy of R^2 = 0.88 with low error metrics (RMSE = 3.48% and MAPE = 2.35%). Additionally, the findings indicated that the highest rice yields (8.21-8.36 tons/ha) were observed at moderate WRC levels (60-75%) compared to other residue percentages. These outcomes suggest that an appropriate amount of WRC enhances rice yield by supporting moisture retention and nutrient availability, which optimizes overall crop performance. Therefore, we strongly recommend that the integration of Gaofen satellite data with NDVI could be a scalable, cost-effective solution for accurate yield prediction that supports sustainable residue management practices and precision agriculture.

Key words: crop residue management; NDVI; precision agriculture; rice mapping; yield prediction.

Introduction

Rice (*Oryza sativa*) is one of the most important crops and is used as regular food for more than three billion people worldwide (Dong and Xiao, 2016). The crop is cultivated in over 100 countries, covering about 164 million hectares and producing 510 million metric tons annually (Dorairaj and Govender, 2023). Recently, the U.S. Department of Agriculture (USDA) forecasted that the initial production of rice for the 2023/24 season would hit a record 520.5 million tons, representing a notable increase of 12.1 million tons compared to the previous year. However, China is one of the world's largest producers and consumers of rice (Guo *et al.*, 2017), with a production of 208.49 million tons in the year 2023 (National Bureau of Statistics of China, 2023). Despite the extensive area under rice cultivation and significant production worldwide, the total demands often exceed supply, with consumption projected to be 530 million tons in 2030 (Durand-Morat and Bairagi, 2021).

This increase is driven by the expected to be more than ten billion in 2050, necessitating more production, while climate change further puts massive pressure on the global food demand. To address these challenges, it is important to adopt reliable methods for ensuring long-term sustainable rice crop yields. However, the retention of crop residue or straw plays an important role in replenishing soil nutrient stocks, increasing rice yield, improving soil structure, and enhancing soil total nitrogen (TN), available phosphorus (AP), and organic matter (OM) (Memon *et al.*, 2018). Accordingly, the estimation of crop yield forecasting under different amounts of preceding crop residue is critical for providing reliable information to decision-makers, helping them develop policies to address food security

challenges in cases of shortfall or surplus (Van Dijk *et al.*, 2021) under conservation agricultural practices (Guo *et al.*, 2023). Traditionally, crop yield information data has been gathered through agricultural statistics, which rely on large-scale field surveys and farmer interviews. Despite its invaluable role in understanding historical trends in rice cultivation, these techniques are time-consuming, imprecise, and labor-intensive (Wu *et al.*, 2014), also the yield data is typically released to the stakeholders and government agencies several months after the crop has been harvested, and thus making it less useful for food security planning.

Meanwhile, in recent years, RS-based techniques have rapidly provided land surface information across large areas, and with an increment in temporal and spatial resolution, satellite data is now freely available (Raza *et al.*, 2024). The benefits of RS technology, such as efficient analysis and spatial coverage over a regional agroecosystem, are significant; it is available year-round at a relatively low cost through freely available optical and multi-temporal satellites**,** such as Landsat, Sentinel, Gaofen, and MODIS. These satellites provide timely information and are capable of mapping detailed spatial distributions of different cropping regions. Moreover, for effective rice crop monitoring and yield estimation, remote sensing images are captured throughout the growing season at the critical growth stages (*e.g.*, transplantation, tillering, panicle initiation, flowering). These images are then analyzed using NDVI to assess vegetation dynamics and predict yield outcomes. The NDVI values are initially low during the transplantation stage, progressively increasing through the vegetative and reproductive phases and gradually declining as the crop progresses towards the ripening phase (Figure 1).

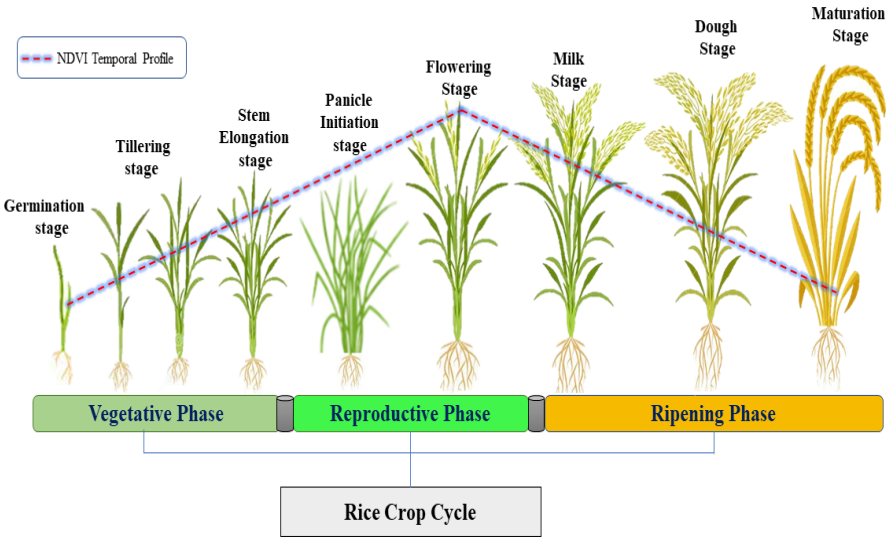

Figure 1. Illustration of rice growth cycle with different phases and stages. Blue-dotted line represents a temporal profile of NDVI associated with the growing stages of rice crops. (Modified after Mosleh *et al.*, 2015; Aguilar, 2019; with permission).

As the rice crop grows through different phenology, its reflectance characteristics change across spectral wavelengths. Several vegetation indices (VIs) have demonstrated a strong correlation with rice evolution parameters. Additionally, most studies have concentrated on utilizing advanced sensors or combining varying sensors to access land surfaces. Only a limited number of studies have explored using more than two satellite sensors to identify crop types through change detection features in a time series. Liu *et al*. (2018) used multi-temporal data of Landsat-8 (OLI-TIRS), Sentinel-1a (MSI), and Sentinel-2b (MSI), combined with Random Forest (RF) algorithm to classify forest types, highlighting that integration of multi-spectral images can produce suitable results.

Furthermore, China Aerospace Science and Technology Corporation launched a series of satellites under the Gaofen mission equipped with different optical and microwave sensors with distinct characteristics. Specifically, within this mission (Chen *et al.*, 2024), two of the most important and high-resolution satellites primarily used for agricultural and forestry applications are Gaofen-1 (GF-1) and Gaofen-6 (GF-6). Consequently, fine-resolution satellite data alone is often insufficient for timely land surface analysis across such an extensive region. The integration of both GF-1 and GF-6 satellites is providing higher temporal resolution, enabling continuous agricultural monitoring at a regional scale. The main advantage of Gaofen satellites over other sensors, such as Landsat and Sentinel, is their combined higher spatial and temporal resolution. Moreover, the wide-angle sensors of Gaofen-1 and Gaofen-6 (800 km swath at 16 m resolution) allow for broader coverage, making them highly suitable for large-scale agricultural applications and frequent crop monitoring. This capability facilitates time series analysis and increases the likelihood of regular surface observations.

In the present study, a satellite-based approach was developed to map and assess the yield performance of rice crops using RS vegetation indices. Thus, the specific objective of the current research was to integrate the capabilities of Gaofen-1 and Gaofen-6 satellites to develop a model for monitoring and estimating the rice crop yield under different percentages of wheat residue cover (WRC) during the growing season. This study is particularly significant as it enhanced rice crop mapping through the use of multi-sensors and multi-temporal data, which provides valuable insight for crop planting adjustment and yield performance under varying WRC percentages in large agricultural regions.

Materials and Methods

Overview of study site

The research site is situated in one of the primary rice-wheat cropping regions, in Changshu County (31°39′54″N; 120°49′19″E) within the administration of Suzhou district in Jiangsu Province, P.R. China (Figure 2). The area lies within the Tai-Lake plain, part of the Yangtze

River delta, spanning 1,276 km^2 of which 386 km^2 consists of water bodies. The total arable land is 42,265 hectares, including 27,451 hectares of rice, 5,600 hectares of irrigated, and 9,214 hectares of dry land (Memon *et al.*, 2023). This region features a subtropical monsoon climate, with a mean annual temperature of 16 °C, and average yearly precipitation of 1,200 mm. The mean annual number of sunshine hours is 2,000, corresponding to 46% sunshine per year (Chen *et al.*, 2022). However, the dominant cropping system is rice (9.355 tons/ha) and wheat (5.03 tons /ha), along with some other agricultural products such as sorghum, maize, cocoon, vegetables, fruits, and medical herbs supported by abundant water resources.

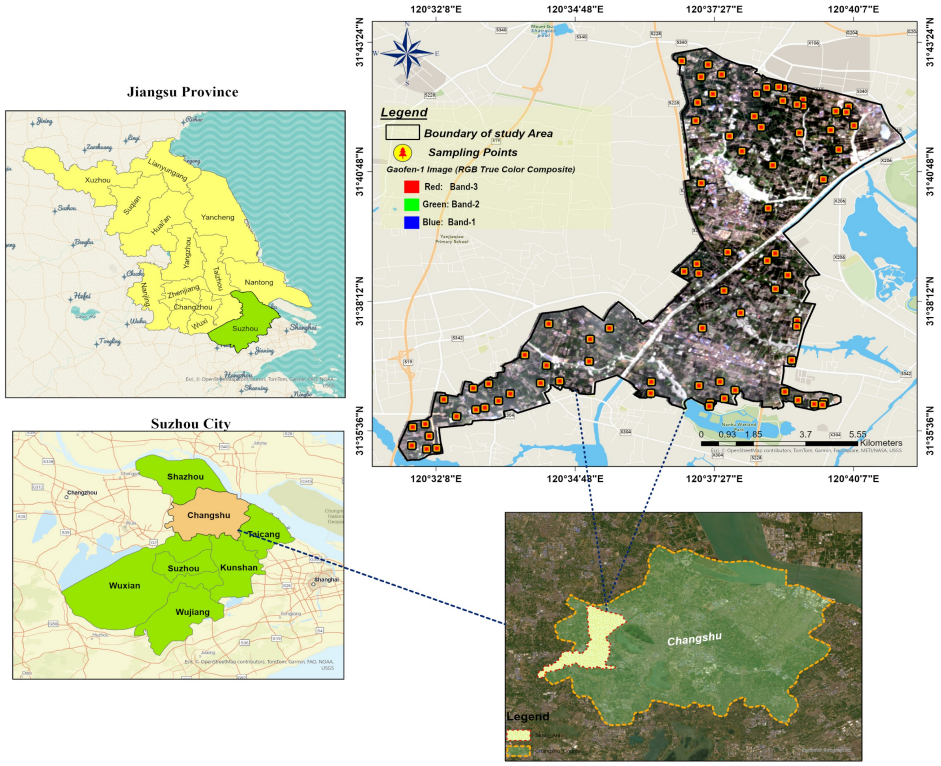

Figure 2. Study area location map with observation points on a Gaofen-1 (GF-1) satellite image (1st August 2019), displayed in a natural color composite: red (B3 band), green (B2 band), and blue (B1 band) of rice growth cycle with different phases and stages.

Field survey and measurement data

A GNSS (Global Navigation Satellite System) based survey and field visit were conducted across 80 paddy fields within the study area during the key stages of rice crop, from June 16 to November 30, 2019. The geographic distribution of location data points is depicted in Figure 2. However, the points were consistent with those utilized to access the wheat residue cover (WRC) percentages in our previous study, where the WRC levels were measured through the line transect method (Memon *et al.*, 2023). Each sampled field spanned an area

of about 1500 m^2 and showed relatively uniform homogeneity. Moreover, in the current study, we utilized the wheat straw cover (WSC) data from our previously developed model, which accurately estimated using Sentinel-2 satellite imagery through Normalized Difference Tillage Index (NDTI), achieving a coefficient of determination (R^2) of 0.85 and an RMSD of 6.49%. The measured rice crop yield and WRC percentage of each sampling point are presented in Table S1.

Collection of secondary data for rice yield model

In addition to the measured rice crop yield obtained from our field observation, we also collected annual production data from a secondary source, specifically the Statistical Yearbooks of Changshu District, Suzhou, 2020 (Statistics, 2020), which served as a crucial benchmark for analysis. These statistical data were employed to develop and refine the algorithm model, which aimed to precisely determine rice yield performance under various wheat residue cover percentages by integrating multisource Gaofen satellite data over a large scale.

Remote sensing data

Remote sensing (RS) offers a reliable method for assessing crop yield performance over large areas under different amounts of residue coverage percentage using various RS-based indices (Memon *et al.*, 2019). In the present study, multispectral data (Figure 3) Gaofen-1 (Xin, 2013) and Gaofen-6 satellites were utilized to estimate rice crop yield. The Gaofen (GF) is a series of Chinese civilian RS satellites developed under the state-sponsored China High-definition Earth Observation System (CHEOS) program. In particular, the GF-1 satellite is a crucial part of China's High-Resolution Earth Observation System and is specifically designed for detailed monitoring of vegetation and forests, inland water surveillance, and exploration of mineral resources. It has a multispectral wide-field-of-view camera sensor with four bands at a 16-meter spatial resolution. Meanwhile, the Gaofen-6 satellite is also primarily used for precision observation of agriculture, forestry resource surveying, and other industries.

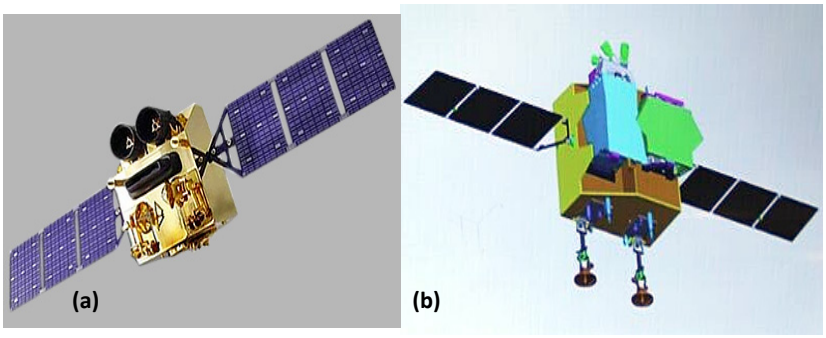

Figure 3. View of the deployed Gaofen satellites spacecraft: a) GF-1 and b) GF-6. Source: Krebs, 2022, 2023.

However, Gaofen-6 has multispectral capabilities with eight bands at a 16-meter spatial resolution, and the temporal resolution of both satellites is four days, which allows for frequent monitoring of crop conditions. Additionally, these satellites' digitization footprint, expressed in data volume, varies according to sensor resolution; the GF-1 satellite's sensors generate approximately 0.000745 MB/ha for multispectral data (Eoportal.org, 2024). This manageable digitization footprint and available efficient processing tools simplify large-scale data handling and facilitate rapid agricultural data analysis. Gaofen satellite images (Level-1A) product were obtained from the China Resources Satellite Data and Application Center platform, accessible at https://data.cresda.cn/#/home (retrieved on 10 August 2024), and technical specifications of these satellites are detailed in Table S2.

Image acquisition

The study utilized GF-1 and GF-6 satellite images acquired during the rice growing season under different straw coverage percentages in the study area. The image acquisition dates were strategically selected with key phenological stages of the rice crop, such as the germination, heading, and grain-filling stages, which are critical for yield performance determination. A total of nine multispectral images (Table 1 and Figure S1) with minimal cloud cover were acquired from both the GF-1 and GF-6 satellites during the June to December 2019 period to assess the rice crop's performance.

Table 1. Summary of GF-1 and GF-6 satellite images acquired during the rice crop season.

No.	Image Capture Dates	Platform	Sensor	Day of Year (DOY)	Scene Cloud Cover
1.	5-June-2019	GF-1	WFV	156	1%
2.	1-Aug-2019	GF-1	WFV	213	2%
3.	21-Aug-2019	GF-1	WFV	233	3%
4.	13-Sep-2019	GF-6	WFV	256	6%
5.	23-Sep-2019	GF-1	WFV	266	2%
6.	19-Oct-2019	GF-6	WFV	292	3%
7.	11-Nov-2019	GF-6	WFV	315	0%
8.	28-Nov-2019	GF-6	WFV	332	3%
9.	6-Dec-2019	GF-6	WFV	340	0%

Processing of satellite images

All the acquired scenes from both satellites (GF-1 and GF-6) were processed using various

preprocessing methods, including geometric correction, radiometric calibration, and atmospheric correction (Ding *et al.*, 2023), implemented with ENVI 5.3 software as per standard procedures. However, the procedure for producing surface reflectance required completing the radiometric calibration for data of Gaofen-1 and Gaofen-6 WFV images, which involves converting the digital numbers to radiance values. After deriving the radiance, top-of-atmosphere (TOA) reflectance was calculated using radiative transfer principal and calibration coefficients, with solar radiance data collected from the metadata of the GF-1 satellite. Moreover, the Level-1A product of Gaofen images required orthorectification correction to ensure the pixels precisely corresponded to the actual ground position in the study area.

Analysis of vegetation indices (VIs)

Subsequent to all these preprocessing steps, a suite of established vegetation indices was derived from the multispectral satellite data to analyze various aspects of rice crop performance parameters. Estimating the rice crop yield under different amounts of WRC coverage involved utilizing a set of well-developed vegetation indices (VIs) calculated from multispectral satellites (He *et al.*, 2016; Memon *et al.*, 2019; Wang *et al.*, 2019) with the integration of GF-1 and GF-6 data (Wang *et al.*, 2017), including i) normalized difference vegetation index (NDVI), ii) enhanced vegetation index (EVI), and, iii) green normalized difference vegetation index (GNDVI). However, NDVI (Rouse *et al.*, 1974) was developed in 1974 and is one of the most commonly used indices for assessing crop characteristics. In contrast, EVI (Liu and Huete, 1995) is a modified version of NDVI that minimizes the influences of soil and atmospheric conditions and improves the sensitivity of high-vegetation areas (Xue and Su, 2017). In addition, the GNDVI (Viña *et al.*, 2011) was also employed in various research to assess the crop condition and technically measures the ratio of reflection from the green and near-infrared wavelengths, which is sensitive to changes in leaf chlorophyll and nitrogen content, a critical factor for crop yield performance (Yang *et al.*, 2011; Xue and Su, 2017) and determined the complementary information about the physiological status of the rice crop under varying soil levels. Moreover, the selected vegetation indices (VIs) used in the present study are illustrated in Table 2.

Table 2. Selected optical vegetation indices for crop yield performance.

Vegetation Index	Abbreviation	Satellites (GF-1 & GF-6)	Reference
Normalized difference vegetation index	NDVI	(B4 – B3)/(B4 + B3)	(Rouse *et al.*, 1974)
Green Normalized Difference Vegetation Index	GNDVI	(B4 – B2)/(B4 + B2)	(Gitelson *et al.*, 1996; Hunt *et al.*, 2013)
Enhanced Vegetation Index	EVI	EVI = G * ((B4 – B3) / (B4 + C1 * B3 – C2 * B1 + L))	(Liu and Huete, 1995)

The coefficients adopted in the MODIS-EVI algorithm are; L=1, C1 = 6, C2 = 7.5, and G (gain factor) = 2.5, ^ For intermediate vegetation cover, L = 0.1, and this value is used most widely.

Afterward, the selected vegetation indices were calculated for each Gaofen satellite image through a comprehensive analytical process (Figure S2) using the ArcGIS Pro Model Builder tool (ESRI, 2014). The key processing phases include a) importing the preprocessed Gaofen imagery, b) extracting and applying VIs bands across the study area, c) Vegetation indices analysis, and d) extracting results into a spreadsheet for further processing. This automated tool was designed to process and determine different indices values for each satellite imagery scene.

Development of model and data analysis

To establish and validate the relationship between the calculated RS-based indices with measured WRC percentage and actual rice crop yield, a total of 80 samples were gathered across the study area. These Samples represent a range of rice crop production under different straw cover percentage levels. Thus, this study developed the predictive crop yield model with randomly separated samples in training and testing datasets, where the training dataset contained 65% (52 Nos) samples; meanwhile, the remaining 35% (28 samples) were allocated for testing dataset to validate the model's performance and assess the consistency between the measured and predicted crop yield. The statistical details for each dataset used to predict crop production are shown in Table 3.

Table 3. Summary statistics of training and testing datasets for rice yield model development.

Dataset	Number of Samples	Crop Yield (kg/ha)			Standard Error (SE±)
		Max	Min	Average	
Training dataset (65%)	52	8,300	6,530	7,688	59.63
Testing dataset (35%)	28	8,250	6,500	7,628	80.01

These datasets used various univariate regression models (Linear and non-linear), including linear, polynomial, and exponential functions (Equation 1 to 3), to establish empirical models through RS-based vegetation indices derived from GF satellite data, along with field measurements of rice crop yield and additional secondary data.

Linear Regression:

$$Y = \beta_0 + \beta_1 X + \text{Ú} \quad \text{(Eq. 1)}$$

where,

Y represents the dependent variable (outcome),
X denotes the independent variable (predictor),
β_0 indicates the intercept, which is the value of Y when $X = 0$,
β_1 = represents the slope (the change in Y for a one-unit change in X) and
Ú= denotes the error term

Polynomial Regression:

$$Y = \beta_0 + \beta_1 X + \beta_2 X^2 + \beta_3 X^3 + \cdots + \beta_n X^n + \text{Ú} \quad \text{(Eq. 2)}$$

where,

Y represents the dependent variable (outcome),
X is the independent variable (predictor),
β_0 indicates the intercept (the value of Y when X =0),
$\beta_1, \beta_2, \ldots.. \beta_n$ represent the coefficients for the polynomial terms, which determine the contribution of each degree of X to the model,
$X^2, X^3, \ldots\ldots, X^n$ are the higher-degree terms (i.e., squared, cubic, etc.), which allow the model to capture non-linear relationships and

U denotes the error term, accounting for the residuals between the observed and predicted values of Y.

Exponential Regression Model:

$$Y = \beta_0 e^{\beta 1X} + \acute{U} \quad \text{(Eq. 3)}$$

where
Y denotes the dependent variable (outcome) being modeled,
X is the independent variable (predictor),
β_0 indicates the scaling coefficient, which is the value of Y when X =0,
e is Euler's number (approximately 2.71828), the base of the natural logarithm,
β_1 represents the rate of growth or decay, which is the exponent coefficient controlling the exponential change of Y with respect to X and
U is the error term

The performance of these models was evaluated using standard statistical metrics, such as the coefficient of determination (R^2), root mean square error (RMSE), and mean absolute percentage error (MAPE). Additionally, the collected field survey data were analyzed using SPSS software (IBM Corp., 2015). The following Equations calculate the RMSD and MAPE (Willmott and Matsuura, 2005);

$$RMSE = \left(\frac{\sqrt{\frac{1}{n}\sum_{i=1}^{n}(x_i - y_i)^2}}{\frac{1}{n}\sum_{i=1}^{n} y_i} \right) \times 100 \quad \text{(Eq. 4)}$$

$$\text{MAPE} = \frac{1}{n}\sum_{i=1}^{n}\left(\frac{x_i - y_i}{x_i} \right) \times 100 \quad \text{(Eq. 5)}$$

where
n the total number of observations,
x_i represent the measured values and
y_i denote the model-predicted values

Software

All the remote sensing image processing, analysis, and modeling were performed using ENVI 5.3, Global Mapper, and ArcGIS Pro 2.7 software.

Results and Discussion

Analysis of field data

The field data collected during the 2019-2020 rice cultivation season were analyzed to assess the variability of rice crop yield under different percentages of wheat residue cover. The WRC percentage was obtained from our previous study (Memon *et al.*, 2023) from 80 sampling fields. The Table S1 data indicated that the highest recorded WRC was 90%, and the lowest was higher or equal to 25% in the study area. Whereas, for the field data analysis, the sampling points were divided into a calibration and validation dataset, which was then used to develop the regression models.

Mapping and classification of paddy fields

The mapping and classification of paddy fields at different stages within the study area were derived from Gaofen satellite imagery (Figure 4). The results indicated that the rice fields were strongly correlated with the previous land use and land cover data and confirming the kappa accuracy of the classification mapping with an overall accuracy of 88% ($\kappa = 0.84$), which is thought to be in accordance with the multispectral satellite data (Shan *et al.*, 2017). However, the classification results revealed distinct spatial patterns across four major land cover classes, i.e., early rice crop class was found the most dominant and covered 38% (2,765 ha), followed by late rice crops at 28% (1,987 ha), urban areas at 25% (1,834 ha) and water bodies at 9% (647 ha) based on the Gaofen NDVI values derived from the satellite imagery acquired on 1st August 2019 (213 DOY). These spatial patterns suggest a predominant focus on rice cultivation, which could be influenced by local agricultural practices and climatic conditions. Whereas urban areas and water bodies occupy smaller portions of the area, they play key roles in delineating the study region's boundaries and usable agricultural land. Moreover, the spatial distribution of rice cropping fields confirmed that the Gaofen multispectral data and NDVI vegetation index could be suitable for mapping and classifying cropping stages at field scale (Song *et al.*, 2017). These findings of rice classification are in agreement with similar research by Jia *et al*. (2022), who employed time-series GF-1-WFV images to construct NDVI to capture crop phenological stages and achieved an impressive classification accuracy of 94.39% with a Kappa coefficient of 0.93 and demonstrated successfully monitoring and mapping of rice crops through NDVI over large areas using Gaofen satellite data.

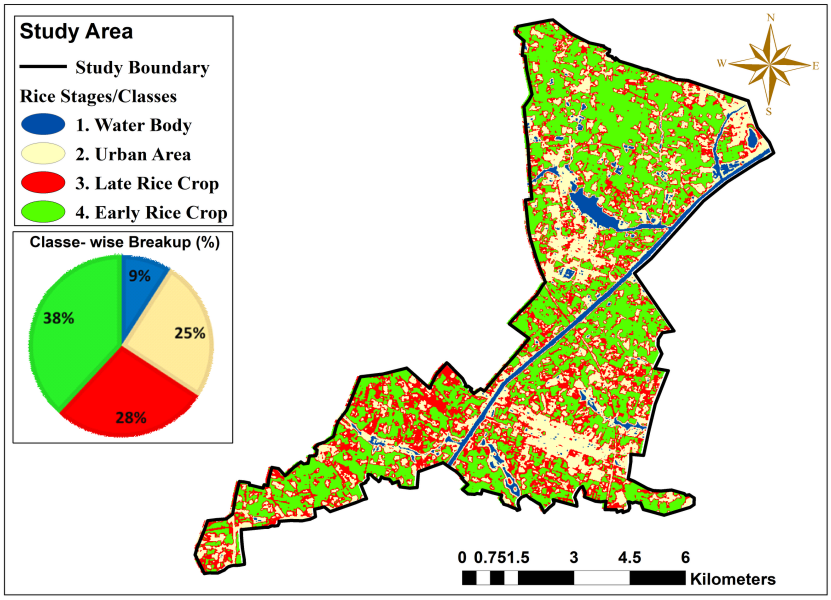

Figure 4. Spatial distribution and classification of rice crop at different stages.

Performance of Gaofen (GF) satellite-based vegetation indices under different residue coverage

Evolutionary trends in normalized difference vegetation index (NDVI)

The temporal profile of NDVI during the rice growing at various growth stages as derived from Gaofen satellite data (Figure 5) and results indicated that the value of NDVI gradually increased from the early stage in June 2019, reaching higher values during the vegetative growth phases, particularly in the month of August and September 2019. However, the highest NDVI value was observed on Day of Year (DOY): 266, with a maximum of 0.835, reflecting the peak greenness and biomass accumulation during the heading and flowering stages of rice development. Prior to this, a significant rise in NDVI was recorded between DOY: 213 and DOY: 233 as the rice crop transitioned through its critical tillering phase. Following this peak, a notable decline in NDVI value occurred as the crop entered the ripening phase, with values dropping from 0.640 to 0.0.573 by DOY: 292 to DOY: 315, respectively.

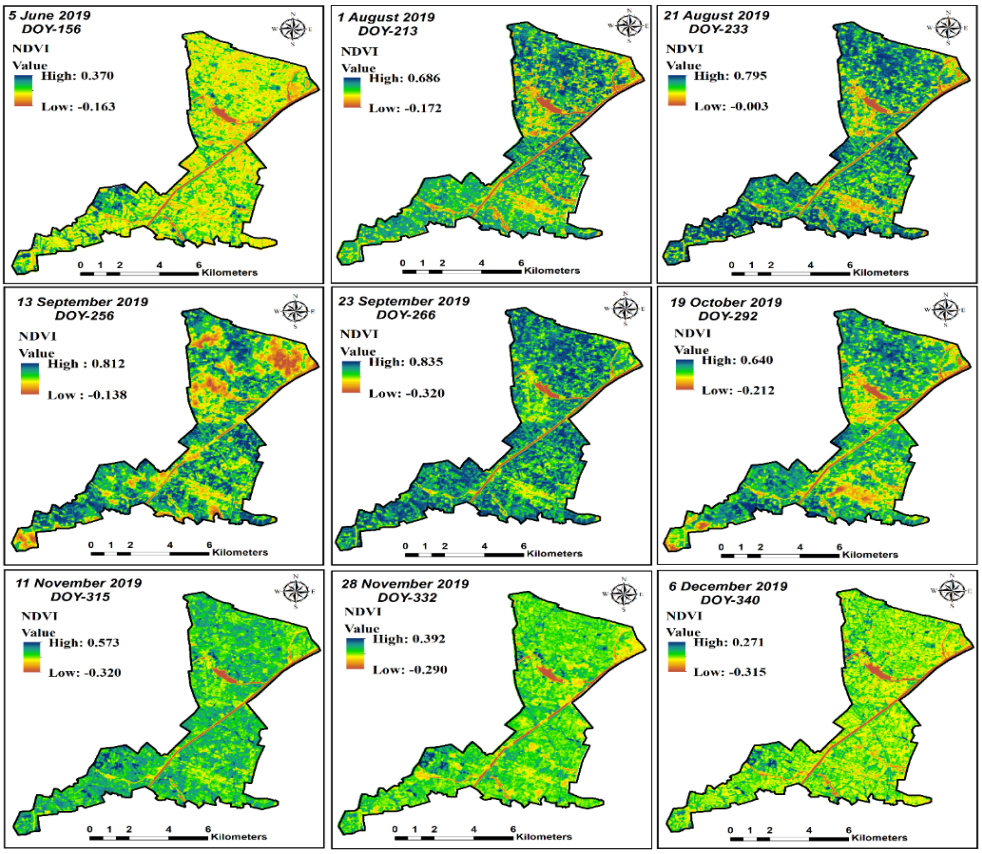

Figure 5. Temporal evolution of NDVI during the rice growing season through Gaofen satellite.

This reduction continued into the post-harvest period, with NDVI values falling to 0.392 and 0.271 on DOY: 332 and DOY: 340), respectively, indicating the maturating stage or end of the crop cycle. Hence, the spatial distribution of NDVI values aligns well with the natural progression of rice growth stages, from germination to harvest. In addition, the relationship between the early and late rice varieties with the NDVI plot (Figure 6) highlighted that the early rice variety consistently exhibited higher NDVI values than the late rice variety throughout the growth stages. At the initial stage (DOY 156), early rice had an NDVI value of 0.320, while late rice was at 0.265. During the peak growing period (DOY 266), the value was recorded as 0.815 and 0.750 for early and late rice, respectively. After the peak, both varieties entered the ripening phase, with NDVI values decreasing from 0.620 (early rice) to 0.650 (late rice) on DOY 292. Subsequently, during the post-harvest stage, early rice values dropped to 0.390 on DOY 332 and further declined to 0.258 on DOY 340, while late rice followed a similar trend, declining from 0.450 to 0.290 in the same period. The trend demonstrated that early rice reached its maximum greenness slightly earlier than late rice, although both followed a similar pattern with the natural progression of rice growth stages, from germination to harvest.

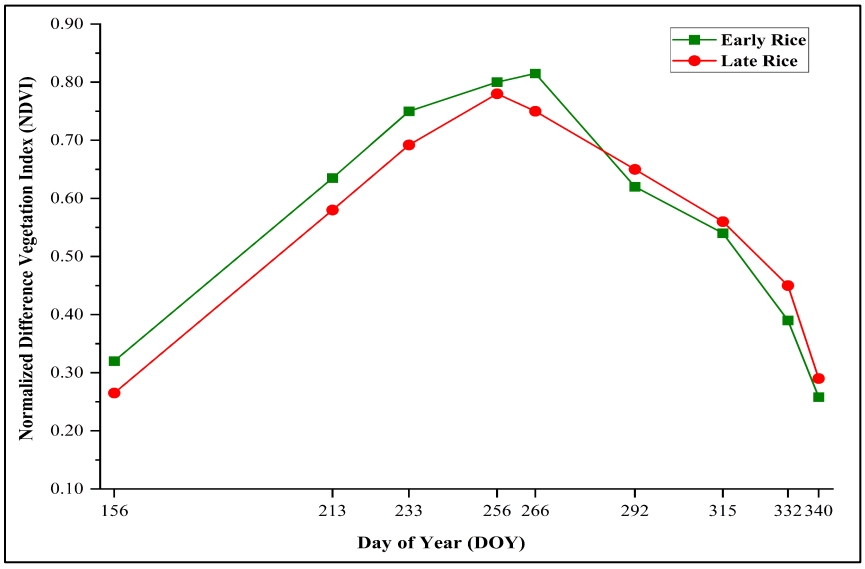

Figure 6. Temporal variation of NDVI for early and late rice varieties.

Overall, the present study findings are supported by previous studies of Wang et al. (2017), who used GF-1 imagery data and NDVI vegetation index to monitor rice growth stages, showing a strong correlation between cumulative NDVI and aboveground biomass with an R^2 value of 0.85. Also, Luo *et al*., (2021) reported that the high accuracy of NDVI-based crop classification, owing to the high spatial and temporal resolution of Gaofen satellites, allows for more precise monitoring of crop phenological stages. Additionally, Shan *et al*. (2021) indicated that GF-6 satellite data could achieve an accuracy of 77.85% in paddy rice areas by using a combination of NDVI index during crop season. Therefore, our results validate and confirm that multi-temporal data of GF-1 and GF-6 satellites combined with NDVI is an effective tool for providing timely data on rice crop conditions, optimizing yield outcomes, and monitoring rice crop growth parameters, particularly under different residue cover percentages on crop yield at regional scale.

Evolution of enhanced vegetation index (EVI)

Temporal time-series of the enhanced vegetation index (EVI), derived from Gaofen data (Figure 7), indicated that the EVI values were relatively low (0.304) on DOY-156 due to early crop development and limited canopy cover, then gradually increased to reach 0.594 by DOY-213 during the active vegetative stage. However, the highest EVI value was observed at 0.772 on DOY-266, which corresponds to maximum canopy cover and biomass during the heading and flowering stages. Following this, the EVI values declined as the crop matured and entered the ripening phase, with further reductions to 0.686-0.312 on DOY

292 and DOY 332, respectively. In comparison, the lowest EVI value was recorded at 0.285 on DOY-340, demonstrating the senescence stage. These trends demonstrate the capability of EVI, captured through Gaofen satellite data, to monitor key phenological stages, with variations under different straw coverage percentages highlighting the influence of residue management on canopy dynamics. Our results are supported by the findings of Wang *et al*. (2017), who demonstrated the effectiveness of the enhanced vegetation index (EVI) derived from Gaofen-1 satellite data in monitoring rice crop growth and estimating yield and found that the quadratic polynomial regression model achieved a high coefficient of determination (R^2 = 0.95) and a relative cross-validation root mean square error (RRMSE) of 54.27, the study further suggested that EVI with Gaofen data illustrating the capability to reflect rice growth dynamics throughout the season accurately.

Similarly, Luo *et al*. 2021 confirmed that EVI derived from GF-1 and GF-6 satellites accurately captured rice crop dynamics, achieving a classification accuracy of 94.1%. These results are in agreement with our findings, confirming that the high temporal and spatial resolution of GF-1 and GF-6 imagery combined with EVI can accurately assess and monitor rice phenology and estimate crop yield. The consistency across these studies reinforces the suitability of Gaofen satellite imagery and EVI for precision agriculture, particularly in rice yield estimation under different residue covers.

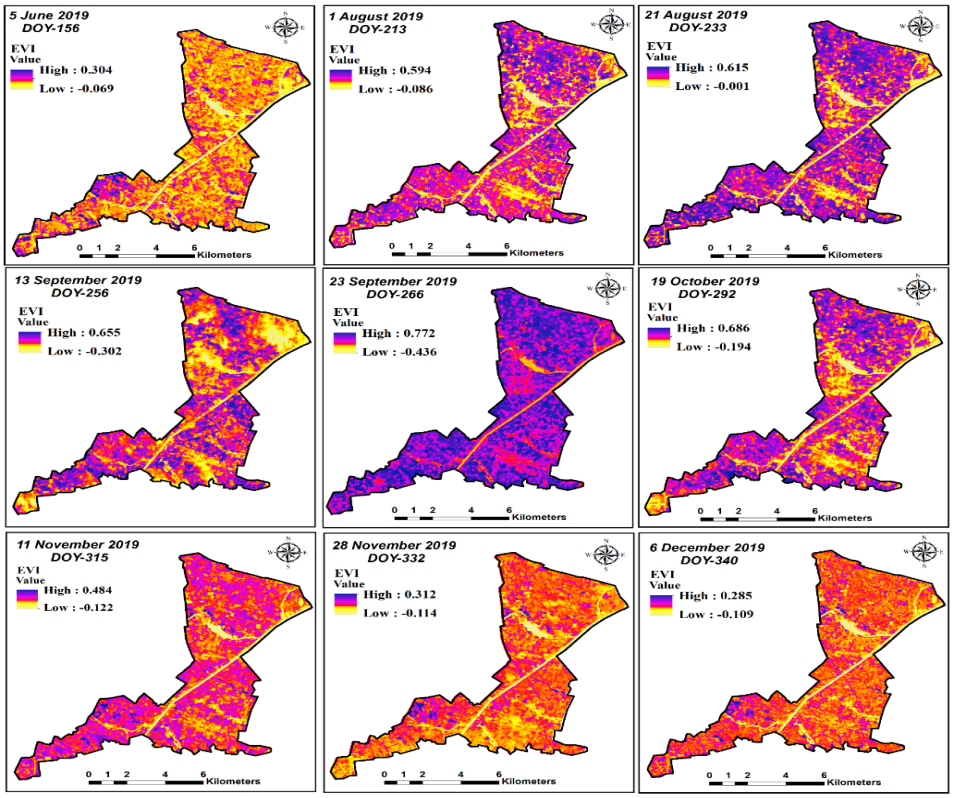

Figure 7. Temporal evolution of EVI using Gaofen satellite data during the rice growth season under different straw cover percentages.

Evolution of green normalized difference vegetation index (GNDVI)

Figure 8 presented the temporal variation of the GNDVI from Gaofen imagery during the rice growing season. The values of GNDVI fluctuate significantly over the development of the crop growing season, reflecting various phases of the rice crop's growth cycle and the impact of crop residue coverage on the chlorophyll content and overall health. The results demonstrated that GNDVI values were relatively low (0.572) on DOY-156, which corresponded to the initial crop development when leaf area and chlorophyll content were still limited. However, the GNDVI values increased steadily from DOY-213 to DOY-233 at 0.687 and 0.735, respectively, which indicates the crop transition to the reproductive phase. The maximum GNDVI value was recorded at 0.810 on DOY-256, reflecting the highest chlorophyll content and optimal conditions for photosynthesis during the heading and flowering stages, where the rice crop exhibited its most robust growth. Following this higher peak, a decline was observed in GNDVI as the crop entered the ripening phase, and the values dropped to 0.597 on DOY-292, signaling the onset of senescence as the rice crop matured. The reduction in GNDVI continued into the post-harvest phase, where values further decreased to 0.516 and 0.312 on DOY-332 and DOY-340, respectively, which reflected the crop senescence stage and substantial reduction in chlorophyll as the crop harvest phase.

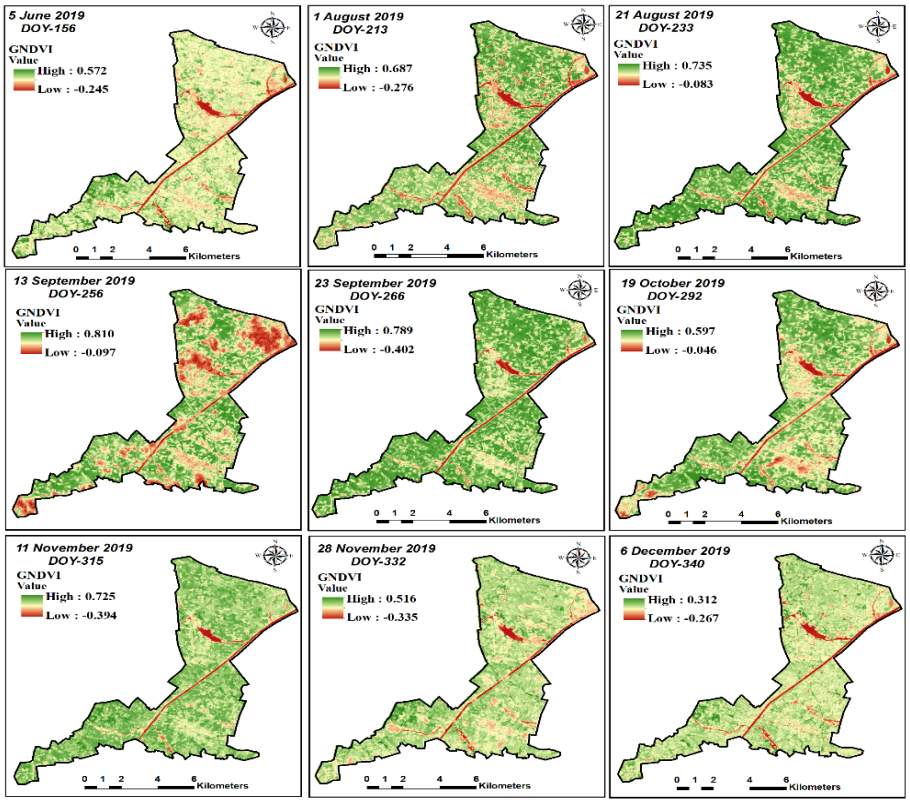

Figure 8. Temporal Progression of GNDVI derived from Gaofen data during the rice growing season.

Moreover, the evolution results of GNDVI of the present study are aligned closely with the natural progression and reflect the dynamic interaction between crop growth stages and the different crop straw coverage. In the early growing season, the relatively low GNDVI values were influenced by soil contact and showed the initial decomposition of straw, which delays nutrient availability. Then the straw decomposes, and the rice canopy develops, where GNDVI values increase and chlorophyll concentrations are at their highest. These findings are corroborated by Ghimire *et al*. (2020), who demonstrated that GNDVI, derived using the Gram-Schmidt fusion method through Gaofen satellite data, was highly reliable in analyzing vegetation characteristics and crop yield estimation, achieving a correlation coefficient of 99.03% and a root mean square error of 10.06%. Their results confirmed the robustness of GNDVI in reflecting temporal variations in chlorophyll content and canopy structure, which parallels our findings that GNDVI effectively monitors rice crop growth stages and provides reliable crop yield estimates. Similarly, Yuan *et al*. (2023) reported that GNDVI derived from Gaofen-6 data achieved a classification accuracy of 87.89%, particularly in distinguishing different crops and growth stages. Additionally, Ali *et al*. (2019) emphasized the sensitivity of GNDVI to spatial variability in crop yields over several years, identifying strong correlations with crop yield during mid-reproductive growth stages, with

correlation coefficients ranging from 0.729 to 0.935, also confirmed that GNDVI provides accurate insights into rice crop condition and yield estimation. Thereby, the consistent results across these studies affirm that GNDVI is a reliable indicator for monitoring crop health and predicting crop yield, reinforcing the utility of Gaofen imagery data for large-scale agricultural monitoring and decision-making in precision agriculture.

Development and performance of rice yield model using integrated GF-1 and GF-6 data

The relationship between the maximum value of vegetation indices (VIs), i.e., NDVI, EVI and GNDVI with measured WRC percentage was analyzed and developed a regression-based model for the sampling data points (n = 80) across the study site, as illustrated in Figure 9. Peak values for each index were recorded during the key growth stage (DOY: 233-266) of the rice crop. The results demonstrated a positive correlation between VIs and WRC, which were strongly fitted in a moderate polynomial regression model, with coefficient of determination (R^2) values of 0.66, 0.60, and 0.51 for NDVI, EVI, and GNDVI, respectively. Among these, the highest NDVI and EVI values were observed at 0.840 and 0.750 for WRC-60%, while the lowest values were found at 0.56 and 0.46 for WRC-20% for NDVI and EVI, respectively. However, the GNDVI values were highest (0.810) at WRC-60% and lowest (0.423) at WRC-25%. This trend in NDVI, EVI and GNDVI indicated that moderate straw cover enhances vegetation greenness, supports chlorophyll retention and is essential for the photosynthesis activity of rice crops.

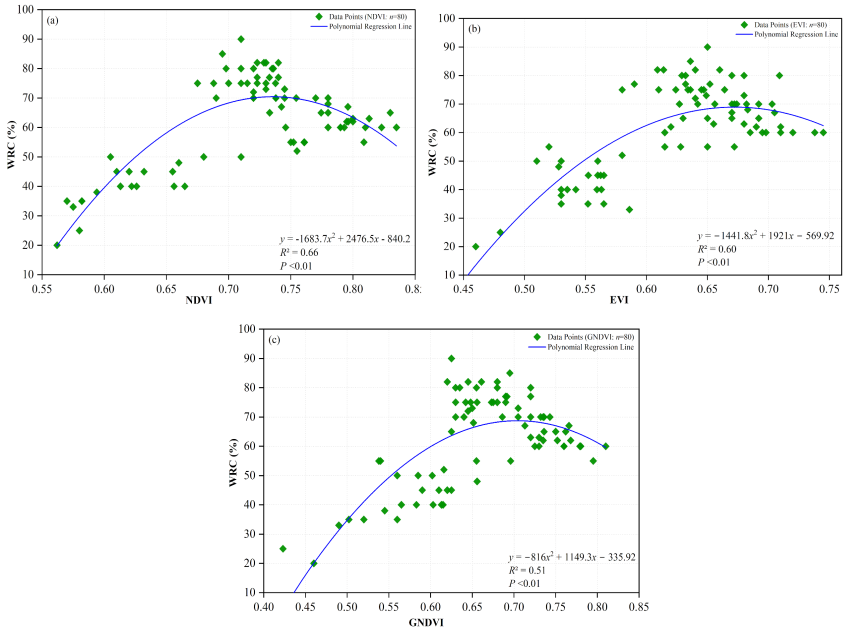

Figure 9. Relationship between vegetation indices and wheat residue cover (WRC) percentage for corresponding sampling points (n=80). (a) WRC with normalized vegetation index (NDVI), (b) Enhanced Vegetation Index (EVI) with WRC and (c) Green Normalized Difference Vegetation (GNDVI) with WRC.

Moreover, the excessive wheat straw cover percentage may limit the emergence rate, affect canopy structure and hinder photosynthetic activity, which potentially stresses plant growth by dense residue cover (Memon *et al.*, 2018; Yadav *et al.*, 2019). The results of our present study for correlation models of crop performance through vegetation indices are closely aligned with the previous study of Memon *et al*. (2019), who highlighted the effectiveness of NDVI in accurately predicting rice crop yields under varying straw coverage through Landsat satellite and their model achieved a positive relationship between the different amount of residue cover and NDVI with R^2 of 0.67 with highest and lowest NDVI values with WSC-68% (0.86) and WSC-33% (0.60), respectively at peak vegetative stages. Additionally, Yaghouti *et al*. (2019) demonstrated that vegetation indices, specifically NDVI and EVI, are highly effective for predicting rice crop yield through different satellite data, particularly when applied during key growth stages of rice crops. The normalized difference vegetation index (NDVI) serves as a strong predictor, with positive correlations to rice yield at the flowering stage, and achieved R^2 for local and high-yield varieties as 0.71 and 0.70, respectively. At the same time, the enhanced vegetation index (EVI) is shown as a precise and effective crop yield estimator, particularly in the context of diverse rice cropping systems of Hunan Provinces, where the initial EVI values were observed at 0.15 at the transplanting stage and rise as vegetation developed.

In contrast, the higher EVI values were found at 0.55 during the heading stage, which is associated with healthier and denser vegetation, often correlating with higher yield potential. Both research findings concluded that NDVI and EVI, tailored to crop growth stages and local conditions, would provide robust and precise remote sensing tools for rice yield estimation. Furthermore, the GNDVI also strongly predicts rice yield, especially when integrated into advanced modeling techniques through multispectral satellite and UAV imagery. A mixed regression model with GNDVI achieved enhanced accuracy in yield assessment by reducing mean absolute error (MAE) to 2.5% compared to conventional models (Yawata *et al.*, 2019). At the same time, another study by Kang *et al*. (2021) incorporated GNDVI with an artificial neural network (ANN) model through UAV-based multispectral imagery in the rice field. The finding illustrated that root mean square error of prediction (RMSEP) ranging from 24.2 to 59.1 kg per 1,000 m^2 across multiple years, which highlighted the GNDVI capability in capturing variations in crop health and significantly determine the effect chlorophyll content and canopy structure due to different levels of fertilizers. Both researches emphasized the reliability of GNDVI as a predictor for analyzing key variations in rice crop health under diverse field conditions, such as differing rice varieties, fertilizer levels, and environmental factors. By this means, it is further recommended that vegetation indices derived from GF-1 and GF-6 satellite data, such as NDVI, EVI, and GNDVI, can effectively be employed to develop precise predictive models

for rice crop performance and yield under varying amounts of wheat residue cover (WRC) percentages. These models provide valuable insights for optimizing residue management practices to maximize crop productivity.

In addition, among the analysis of three vegetation indices, NDVI was chosen for the development of the yield model due to its significant performance (R^2 = 0.66) as compared to EVI (R^2 = 0.60) and GNDVI (R^2 = 0.51) regard to correlation with WRC percentage (Figure 9). However, a linear regression model was developed to establish the relationship between NDVI and measured rice yield using the training dataset (n = 52), as presented in Figure 10. The results indicated a strong positive correlation with R^2 = 0.83, and the highest and lowest values of NDVI were observed, 0.82 and 0.57, to the rice yield of approximately 8,050 and 6,730 kg/ha, respectively. The Equation, derived from the calibration dataset, is given below:

Predicted Yield (kg/ha) = 5600 × NDVI + 3690 (Eq.6)

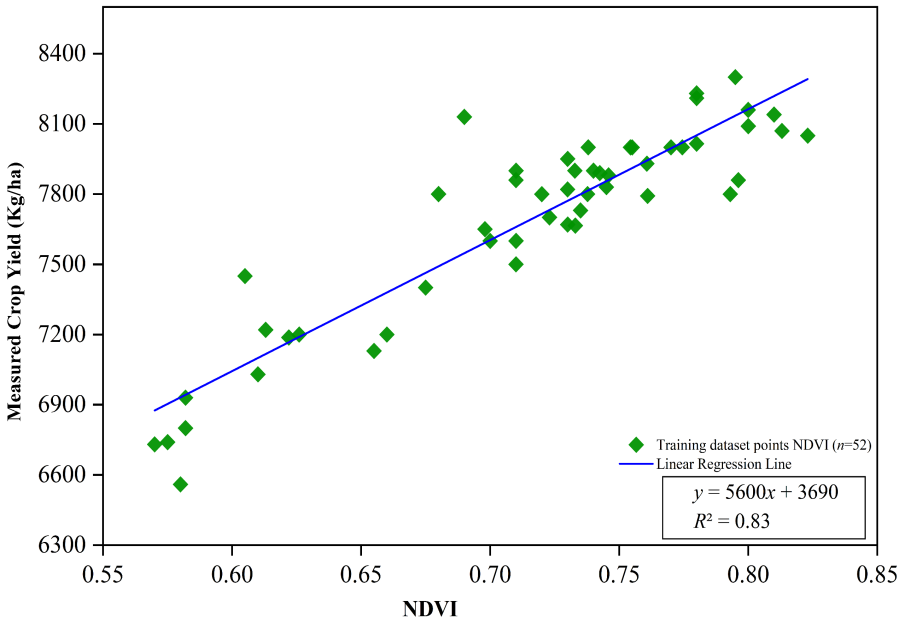

Figure 10. Relationship between NDVI and crop yield under different WRC percentages. "n" denotes sampling points of the training dataset.

These outcomes highlight that NDVI can be effectively used to determine crop health performance and predict rice productivity with considerable accuracy across different WRC conditions. However, the present findings are consistent with previous studies by Singha and Swain, (2022); Siyal *et al*. (2015) revealed that NDVI has a strong predictive capability in estimating rice yield. In their studies, the R^2 values of yield models were achieved at 0.406

and 0.94 with Sentinel and Landsat satellite data, respectively, which reflected the positive correlation between NDVI and rice crop performance. The uniformity of these studies emphasizes NDVI's effectiveness as a considerable indicator for predicting rice yield under varying field conditions.

Estimation of rice yield using developed predictive model

In the present study, the yield estimation model was validated through Equation (6) and employed on the testing dataset (*n*=28) of sampling points to predict rice crop yield with peak NDVI data (Figure 10). The predicted yield data were then compared to the measured data (Figure 11), which were gathered from ground truth surveys and the statistical yearbooks of Changshu District, Suzhou, for 2020-2021 (Statistics, 2020) for the study site.

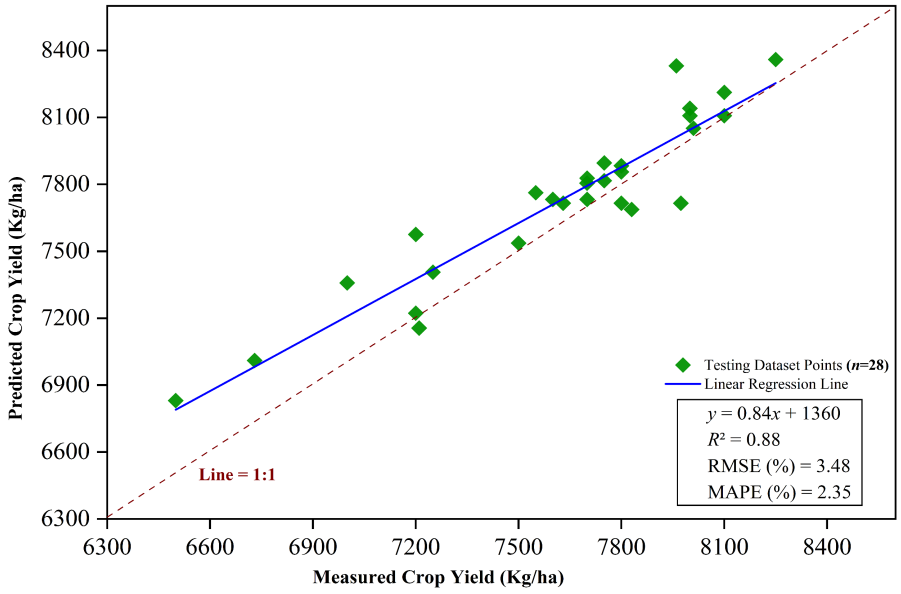

Figure 11. Relationship between predicted and measured rice yields for model validation using NDVI-based regression through the testing dataset (n=28).

However, the yield predictive model was fitted to a linear regression Equation and exhibited a significant positive correlation with the coefficient of determination (R^2) value of 0.88. The RMSE and MAPE for the validation model were 3.48% and 2.35%, respectively, which signified a low margin of error and confirmed the precision of the model in predicting rice yields.

These observations are in agreement with earlier studies by Son *et al.* (2020), who applied RS and machine learning techniques, mainly using NDVI, in predicting crop yields through

satellite data and achieved R^2 values of 0.84 and 0.85 with RMSE of 5.6% and 8.46% respectively, showcasing the model's reliability in rice yield forecasting across different field and environmental conditions. Thus, this strong correlation between predicted and measured yields recommended that the model performs well under varying WRC conditions across the study region.

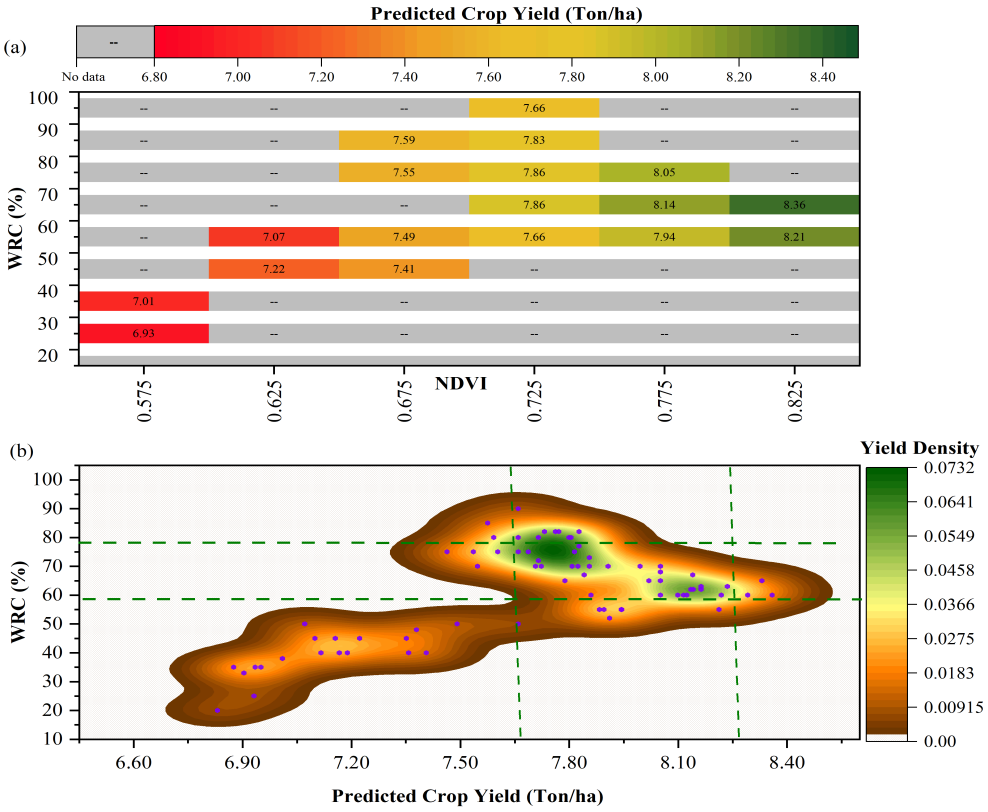

Figure 12. Illustration of the relationship between NDVI and predicted rice crop yield under different percentages of WRC across sampling points (n = 80) in the study area. (a) Split heat map depicting WRC, NDVI, and rice yield; (b) Bivariate kernel density plot of yield distribution relative to WRC percentages.

Subsequently, to determine rice crop production under varying WRC percentages, we utilized Eq. 6 through NDVI values to cover sampling points (n=80) across the study area. We analyzed the relationship between predicted rice yield and WRC coverage percentage, as presented in Figure 12. The split-class heatmap (Figure 12a) indicated that the mean rice grain yields were significantly highest (8.21-8.36 ton/ha) at a WRC level of 60-70%, with NDVI ranging from 0.823 to 0.835. In contrast, the lowest yield was observed, 6.83-7.01 ton/ha at a WRC level of 20%-35%, with NDVI values ranging from 0.562 to 0.600, respectively. However, the kernel density plot (Figure 12b) further revealed the influence of WRC on rice crop yield and showed a high concentration of yield density (0.073) in the mid-range of wheat residue coverage of 60-75%, within the average yields between 7.66 to 8.36 tons/ha compared to other WRC percentage. The outcomes further emphasize that an

appropriate amount of crop residue is beneficial because excessive or minimal straw coverage might inhibit crop health, either with poorer nutrient availability or excessive shading, which ultimately limits soil physicochemical properties and affects the crop emergence rate and yield performance. Moreover, these results are supported by Song *et al*. (2016) prior studies of ho reported that a suitable amount of crop residue coverage is a key management strategy for enhancing emergence rate, seedling growth quality, and grain yield in rice. Similarly, Memon *et al*. (2019) stated that applying wheat straw at different percentages significantly impacts the rice crop yield, with the highest production estimated at 8,439.67 kg/ha under 68% residue coverage. Their analysis also presented a bivariate kernel density distribution and determined higher yield density (0.082) with a mean rice yield of 8.30 to 8.40 tons/ha in the range of wheat residue cover of 65-78%, respectively.
In contrast, the lower yields were recorded with WRC levels below 30%, where yields dropped substantially, reflecting the negative impact of minimal residue amount on soil quality and crop yield. Therefore, the present study's findings underscore the precision and consistency of the yield model developed with the NDVI vegetation index through Gaofen satellite data under various WRC percentages. The insights gained from these visualizations are significant, indicating that moderate WRC levels (60-75%) are crucial for achieving optimal rice yield and providing valuable guidance for precision agriculture practices, emphasizing efficient residue management strategies to enhance higher crop productivity and support long-term sustainable agriculture. Notably, integrating NDVI with high-resolution Gaofen satellite imagery is essential for accurately monitoring rice crop yield performance across large agricultural regions.

Conclusions and suggestions for future research

In this study, an advanced regression-based model was developed to predicate rice yield through the combination of Gaofen-1 and Gaofen-6 satellite data with the utilization of various vegetation indices (VIs) under different wheat residue cover (WRC) percentage conditions under a rice-wheat cropping system. The land use/land cover (LULC) mapping based on Gaofen data demonstrated that paddy fields covered 66% of the study area, achieving an overall classification accuracy of 88% ($\kappa = 0.84$), thus providing a well-defined basis for yield estimation focused on rice cultivation areas, however, by integrating remote sensing-based vegetation indices, including NDVI, EVI and GNDVI, with various WRC percentages for model development, a positive correlation with R^2 values of 0.66, 0.60 and 0.51, respectively, confirming NDVI as the most effective indicator for predicting rice yield. The rice yield model was developed by correlating the peak NDVI values of training sampling points (n=52) with ground-measured rice yield resulting in R^2 =0.83. For model validation, the yield predictive model was tested using a dataset (n=28) and fitted to a linear regression equation, which exhibited a significant positive correlation with high accuracy (R^2=0.88) and low error metrics (RMSE = 3.48% and MAPE = 2.35%). Additionally, the

finding highlighted that the highest predicted grain rice yields were recorded in the range of 8.21-8.36 tons/ha at moderate WRC levels of 60-70%, corresponding to NDVI values between 0.823 and 0.835. The bivariate kernel density plot further confirmed a high concentration of yield density (0.073) within the mid-range of WRC (60-75%) compared to other WRC percentages. This suggests that an appropriate amount of crop residue is beneficial for enhanced crop yield, likely due to improved soil moisture retention and nutrient availability, positively impacting overall crop performance. Therefore, our findings strongly recommend that Gaofen satellite imagery is highly effective for monitoring and estimating rice crop yield across varying WRC percentages. By combining GF data with vegetation indices, this approach offers a scalable, RS-based solution for accurate yield prediction, supporting sustainable agricultural practices and advancing precision agriculture at a regional scale. Moreover, the approach can assist scientists and policymakers in addressing agricultural sustainability challenges and adapting agricultural systems to global climate change, providing valuable insights into food security strategies and resource management. Furthermore, the present study establishes a foundation for future research exploring additional remote-sensing satellite data, multi-year evaluations, and advanced machine-learning techniques combined with vegetation indices under diverse crop types, climate zones, and field management practices. Such efforts will enable a better understanding of assessing the impact of crop residue coverage on crop yield in agroecosystems using remote sensing-based technologies for yield estimation.

Supplementary Materials: The following supporting information is attached in supplementary: Table S1: Measured wheat residue cover (WRC) percentage over the study area; Table S2: Detail of spectral band wavelengths with a spatial resolution for GF-1 and GF-6 satellites; Figure S1: Images acquired from Gaofen-1 and Gaofen-6 satellites for current study during; and Figure S2. Methodology workflow for data extraction through the ArcGIS Pro Model Builder; ROI, region of interest.

Acknowledgments: This research work was supported by the Single Technology Research and Development Project of Jiangsu Agricultural Science and Technology Innovation Fund (CX(23)3032), Key Laboratory of Modern Agricultural Equipment and Technology of Jiangsu University [MAET202118] and Project Funded by the Priority Academic Program Development of Jiangsu Higher Education Institutions, China [PAPD-2023-87]. Additionally, we extend our warm thanks to the landlord and farmer of the sampling points who participated in the ground truth survey and field measurement campaigns in the study area. The first author is also grateful to the China Postdoctoral Science Foundation for

providing Postdoctoral Fellowship# 336849 to pursue research at the School of Agricultural Engineering, Jiangsu University, China.

Contributions: Conceptualization, M.S.M; Data curation, M.S.M. and J.G.; Formal analysis, M.S.M. and B.I.; Funding acquisition, S.C.; Investigation, M.S.M, J.G. and Z.D; Methodology, M.S.M, J.G. and Z.D.; Resources, S.C.; Software, M.S.M, B.I and M.F.T.; Supervision, S.C.; Validation, M.S.M., and N.M.; Visualization, M.S.M, M.F.T and N.M; Writing – original draft, M.S.M.; Writing – review & editing, M.S.M. and S.C.

Conflict of interest: The authors have no conflict of interest to declare.

References

Aguilar, A., 2019. Machine learning and big data techniques for satellite-based rice phenology monitoring. MSc Thesis, University of Manchester.

Ali, A., Martelli, R., Lupia, F., Barbanti, L., 2019. Assessing multiple years' spatial variability of crop yields using satellite vegetation indices. Remote Sens. 11:2384.

Chen, C., Lv, Q., Tang, Q., 2022. Simulating and predicting soil water dynamics using three models for the Taihu Lake region of China. Water Supply 22:4030–4042.

Chen, L., Letu, H., Fan, M., Shang, H., Tao, J., Wu, L., Zhang, Y., Yu, C., Gu, J., Zhang, N., Hong, J., Wang, Z., Zhang, T., 2024. An introduction to the Chinese High-Resolution Earth Observation System: Gaofen-1~7 civilian satellites. J. Remote Sens. 2022:9769536.

Ding, Y., Gu, X., Liu, Y., Zhang, H., Cheng, T., Li, J., Wei, X., Gao, M., Liang, M., Zhang, Q., 2023. GF-1 WFV surface reflectance quality evaluation in countries along "the Belt and Road." Remote Sens. 15:5382.

Dong, J., Xiao, X., 2016. Evolution of regional to global paddy rice mapping methods: A review. ISPRS J. Photogramm. Remote Sens. 119:214–227.

Dorairaj, D., Govender, N.T., 2023. Rice and paddy industry in Malaysia: Governance and policies, research trends, technology adoption and resilience. Front. Sustain. Food Syst. 7.

Durand-Morat, A., Bairagi, S., 2021. International rice outlook: International rice baseline projections 2020–2030. University of Arkansas.

ESRI, 2014. ArcMap 10.2. ESRI, Redlands, California.

Eoportal Directory, 2024. GF-1 (Gaofen-1) Earth Observation Satellite Mission. European Space Agency (ESA). Available from: https://www.eoportal.org/satellite-missions/gf-1

Ghimire, P., Lei, D., Juan, N., 2020. Effect of image fusion on vegetation index quality—A comparative study from Gaofen-1, Gaofen-2, Gaofen-4, Landsat-8 OLI and MODIS imagery. Remote Sens. 12:1550.

Gitelson, A.A., Kaufman, Y.J., Merzlyak, M.N., 1996. Use of a green channel in remote sensing of global vegetation from EOS-MODIS. Remote Sens. Environ. 58:289–298.

Guo, J., Hu, X., Gao, L., Xie, K., Ling, N., Shen, Q., Hu, S., Guo, S., 2017. The rice production practices of high yield and high nitrogen use efficiency in Jiangsu, China. Sci. Rep. 7:2101.

Guo, Y., Cui, M., Xu, Z., 2023. Spatial characteristics of transfer plots and conservation tillage technology adoption: Evidence from a survey of four provinces in China. Agriculture 13:1601.

He, J., Qin, Y., Guo, C., Zhao, L., Zhou, X., Yao, X., Cheng, T., Tian, Y., 2016. Monitoring leaf area index after heading stage using hyperspectral remote sensing data in rice. In: 2016 IEEE International Geoscience and Remote Sensing Symposium (IGARSS). pp. 6284–6287.

Hunt, E.R., Doraiswamy, P.C., McMurtrey, J.E., Daughtry, C.S.T., Perry, E.M., Akhmedov, B., 2013. A visible band index for remote sensing leaf chlorophyll content at the canopy scale. Int. J. Appl. Earth Obs. Geoinf. 21:103–112.

IBM Corp., 2015. IBM SPSS Statistics for Windows, Version 23.0. IBM Corp.

Jia, Y., Zhang, X., Zhang, H., Su, Z., 2022. Crop classification based on a Gaofen 1/Wide-Field-View time series. Eng. Agric. 42.

Kang, Y., Nam, J., Kim, Y., Lee, S., Seong, D., Jang, S., Ryu, C., 2021. Assessment of regression models for predicting rice yield and protein content using unmanned aerial vehicle-based multispectral imagery. Remote Sens. 13:1508.

Krebs, G.D., 2022. Gaofen 6 (GF 6). Available from: https://space.skyrocket.de/doc_sdat/gf-6.htm

Krebs, G.D., 2023. Gaofen 1 (GF 1). Available from: https://space.skyrocket.de/doc_sdat/gf-1.htm

Liu, H.Q., Huete, A., 1995. A feedback based modification of the NDVI to minimize canopy background and atmospheric noise. IEEE Trans. Geosci. Remote Sens. 33:457–465.

Liu, Y., Gong, W., Hu, X., Gong, J., 2018. Forest type identification with random forest using Sentinel-1A, Sentinel-2A, multi-temporal Landsat-8 and DEM data. Remote Sens. 10:946.

Luo, J., Chu, Q., Sun, C., Wang, Y., Sun, D., 2021. Staple crop mapping with Chinese Gaofen-1 and Gaofen-6 satellite images: A case study in Yanshou County, Heilongjiang Province, China. In: 2021 IEEE International Geoscience and Remote Sensing Symposium IGARSS. pp. 6769–6772.

Memon, M.S., Chen, S., Niu, Y., Zhou, W., Elsherbiny, O., Liang, R., Du, Z., Guo, X., 2023. Evaluating the efficacy of Sentinel-2B and Landsat-8 for estimating and mapping wheat straw cover in rice–wheat fields. Agronomy 13:2691.

Memon, M.S., Guo, J., Tagar, A.A., Perveen, N., Ji, C., Memon, S.A., Memon, N., 2018. The effects of tillage and straw incorporation on soil organic carbon status, rice crop productivity, and sustainability in the rice-wheat cropping system of Eastern China. Sustain. 10:0961.

Memon, M.S., Jun, Z., Sun, C., Jiang, C., Xu, W., Hu, Q., Yang, H., Ji, C., 2019. Assessment of wheat straw cover and yield performance in a rice-wheat cropping system by using Landsat satellite data. Sustain. 11:5369.

Mosleh, M.K., Hassan, Q.K., Chowdhury, E.H., 2015. Machine learning and big data techniques for satellite-based rice phenology monitoring. Sensors 15;769-791.

National Bureau of Statistics of China, 2023. Statistical communiqué of the People's Republic of China on the 2022 national economic and social development. Available from: https://www.stats.gov.cn/english/PressRelease/202302/t20230227_1918979.html

Raza, A., Hu, Y., Lu, Y., Ray, R.L., 2024. Comparison of Landsat-8 and Sentinel-2 imagery for modeling gross primary productivity of tea ecosystem. J. Crop Heal. 76:1585–1605.

Rouse, J.W., Haas, R.H., Schell, J.A., Deering, D.W., 1974. Monitoring vegetation systems in the Great Okains with ERTS. Third Earth Resour. Technol. Satell. Symp. 1:325–333.

Shan, J., Qiu, L., Tian, M., Wang, J., Wang, Z., Huang, X., 2021. Study on extraction methods of paddy rice area based on GF-6 satellite image. In: 2021 IEEE International Geoscience and Remote Sensing Symposium. pp. 9530314.

Shan, J., Wang, Z., Sun, L., Yu, K., Qiu, L., Wang, J., Wang, J., Mao, L., 2017. Study on extraction methods of paddy rice area based on GF-1 satellite image. In: 2017 6th International Conference on Agro-Geoinformatics. pp. 8047050.

Singha, C., Swain, K.C., 2022. Evaluating the NDVI based rice and potato yield prediction map using GIS geostatistical environment. In: 2022 Second International Conference on Advances in Electrical, Computing, Communication and Sustainable Technologies (ICAECT). pp. 1–7.

Siyal, A.A., Dempewolf, J., Becker-Reshef, I., 2015. Rice yield estimation using Landsat ETM+ data. J. Appl. Remote Sens. 9:095986.

Son, N.-T., Chen, C.-F., Chen, C.-R., Guo, H.-Y., Cheng, Y.-S., Chen, S.-L., Lin, H.-S., Chen, S.-H., 2020. Machine learning approaches for rice crop yield predictions using time-series satellite data in Taiwan. Int. J. Remote Sens. 41:7868–7888.

Song, K., Yang, J., Xue, Y., Lv, W., Zheng, X., Pan, J., 2016. Influence of tillage practices and straw incorporation on soil aggregates, organic carbon, and crop yields in a rice-wheat rotation system. Sci. Rep. 6:36602.

Song, Q., Zhou, Q., Wu, W., Hu, Q., Lu, M., Liu, S., 2017. Mapping regional cropping patterns by using GF-1 WFV sensor data. J. Integr. Agric. 16:337–347.

Statistics, S.M.B. of, 2020. Suzhou statistical yearbook 2020.

Van Dijk, M., Morley, T., Rau, M.L., Saghai, Y., 2021. A meta-analysis of projected global food demand and population at risk of hunger for the period 2010–2050. Nat. Food 2:494–501.

Viña, A., Gitelson, A.A., Nguy-Robertson, A.L., Peng, Y., 2011. Comparison of different vegetation indices for the remote assessment of green leaf area index of crops. Remote Sens. Environ. 115:3468–3478.

Wang, F., Wang, F., Zhang, Y., Hu, J., Huang, J., Xie, J., 2019. Rice yield estimation using parcel-level relative spectral variables from UAV-based hyperspectral imagery. Front. Plant Sci. 10:1391.

Wang, J., Lu, B., Yu, K., Tian, M., Huang, X., Wang, Z., 2017. Rice growth monitoring using multi-temporal GF-1 images. In: 2017 6th International Conference on Agro-Geoinformatics. pp. 8047018.

Willmott, C.J., Matsuura, K., 2005. Advantages of the mean absolute error (MAE) over the root mean square error (RMSE) in assessing average model performance. Clim. Res. 30:79–82.

Wu, M., Yang, L., Yu, B., Wang, Y., Zhao, X., Niu, Z., Wang, C., 2014. Mapping crops acreages based on remote sensing and sampling investigation by multivariate probability proportional to size. Nongye Gongcheng Xuebao/Trans. Chin. Soc. Agric. Eng. 30:146–152.

Xin, H., 2013. China launches Gaofen-1 satellite. Available from: http://www.china.org.cn/china/2013-04/26/content_28668480.htm

Xue, J., Su, B., 2017. Significant remote sensing vegetation indices: A review of developments and applications. J. Sensors 2017:1353691.

Yadav, G.S., Lal, R., Meena, R.S., Babu, S., Das, A., Bhowmik, S.N., Datta, M., Layak, J., Saha, P., 2019. Conservation tillage and nutrient management effects on productivity and soil carbon sequestration under double cropping of rice in north eastern region of India. Ecol. Indic. 105:303–315.

Yaghouti, H., Pazira, E., Amiri, E., Masihabadi, M.H., 2019. The feasibility of using vegetation indices and soil texture to predict rice yield. Polish J. Environ. Stud. 28:2473–2481.

Yang, Z., Di, L., Yu, G., Chen, Z., 2011. Vegetation condition indices for crop vegetation condition monitoring. In: 2011 IEEE International Geoscience and Remote Sensing Symposium. pp. 3534–3537.

Yawata, K., Yamamoto, T., Hashimoto, N., Ishida, R., Yoshikawa, H., 2019. Mixed model estimation of rice yield based on NDVI and GNDVI using a satellite image. Proc. SPIE 11149:1114918.

Yuan, J., Wu, Z., Li, S., Kang, P., Zhu, S., 2023. Multi-feature-based identification of subtropical evergreen tree species using Gaofen-2 imagery and algorithm comparison. Forests 14:292.